Journal of Biomechanical Science and Engineering

Vol. 2, No. 1, 2007

Numerical Simulation of a Low-Hematocrit Blood Flow in a Small Artery with Stenosis*

Takuji ISHIKAWA**, Nobuyoshi KAWABATA***, Yohsuke IMAI**, Ken-ichi TSUBOTA** and Takami YAMAGUCHI**

**Dept. Bioeng. Robotics, Grad. Sch. Eng., Tohoku University, 6-6-01, Aoba, Aramaki, Aoba-ku, Sendai 980-8579, Japan

E-mail: ishikawa@pfsl.mech.tohoku.ac.jp

***Dept. Fiber Amenity Engineering, University of Fukui, 3-9-1 Bunkyo, Fukui-shi, Fukui-ken 910-8507, Japan

Abstract

The blood flow in a large artery is commonly analyzed by means of constitutive equations. However, it is not appropriate to use these equations for small arteries because of the heterogeneity of the blood. In this study, we use a bead-spring model for an erythrocyte to simulate a low-hematocrit blood flow in a small artery with a stenosis. The flow field is solved using Euler coordinates, whereas the motion of the erythrocyte is solved using Lagrangian coordinates (two-way coupling). The results show that the erythrocytes are considerably deformed around the stenosis and that the separated region downstream of the stenosis is weakened by the erythrocytes.

Key words: Blood Flow, Numerical Simulation, Small Artery, Stenosis, Erythrocyte

1. Introduction

The blood flow in an artery has been widely investigated because the fluid dynamical factor plays an important role in the development of arterial diseases. In considering the non-Newtonian property of the blood, flow fields are commonly analyzed by means of constitutive equations[1-4]. The Casson model[5] is often used as a constitutive equation for the blood; however, it cannot express the elasticity of the blood. Another disadvantage of the constitutive equations is that they are not appropriate for small arteries. In a small artery, the distribution of erythrocytes in the flow field is important, but the constitutive equations assume the homogeneity of the fluid. It is, therefore, hard to explain the basic phenomena of blood flow such as the Fahreaus-Lindqvist effect. To simulate the blood flow in a small artery, it is necessary to compute simultaneously both the erythrocyte motions and the flow field.

The behavior of a single erythrocyte was simulated in detail by Pozrikidis[6-8]. He performed computations for a capsule with a biconcave unstressed shape over an extended range of the dimensionless shear rate and for a broad range of the ratio of the internal to external fluid viscosities. The membrane used in his study is nearly incompressible and exhibits an elastic response to shearing and bending deformation. It requires, however, a high computational load to compute a practical blood flow, in which five million erythrocytes exist per 1 mm^3. Thus, we think that simplifying the erythrocyte model is unavoidable, so that the particle stress tensor in the momentum equation of the blood can be calculated with a realistic computational load.

There are some methods that can efficiently simulate a suspension of rigid particles. Ladd[9-11] was able to carry out Stokesian-dynamics simulations of suspensions with up to 32,000 rigid spheres by a lattice Boltzmann method. Sangani and Mo[12] developed a fast

*Received 12 June, 2006 (No. 06-0040)
[DOI: 10.1299/jbse.2.12]

multipole method (FMM), and carried out Stokesian-dynamics simulations of suspensions with up to 8,000 rigid spheres. Zinchenko and Davis[13, 14] improved the standard boundary element method, and were able to simulate up to 200 deformable drops in a simple shear flow. Some of these methods may be applicable to a suspension of red blood cells, but this has not yet been examined because of the difficulty of dealing with the membrane mechanics.

The authors tried to improve a standard Euler-Lagrangian method for a dispersed two-phase flow, and proposed a bead-spring cell model[15, 16], in which a bead expresses the viscous drag and a spring expresses the elasticity of the membrane. We showed that the model could express the rheological properties of blood, such as the shear-thinning property and the elasticity, and could be useful in solving a blood flow. In this research, a bead-spring model is used for simulating the blood flow in a small artery with a stenosis. We restrict ourselves to low-hematocrit blood in order to avoid *ad hoc* assumption for describing the interaction between cells. The effects of erythrocytes on the flow field and the stress field around the stenosis are discussed.

2. Basic Equations and Numerical Methods

2.1 Erythrocyte model

Most blood cells consist of erythrocytes; therefore, the blood is assumed in this research to be a suspension of erythrocytes and plasma. An erythrocyte is modeled using six drag points and fifteen springs as shown in figure 1. This model is exactly the same as the one proposed by Ishikawa *et al*. (2003) [16], so only a brief explanation will be made here. The drag points express the fluid-dynamical drag force acting on the membrane of the erythrocyte, and the springs express the elasticity of the membrane. It is considered that these two forces dominate the stress tensor contribution of the erythrocyte. In this model, the following four points are assumed: (1) The drag force acting at the drag point is calculated from the drag coefficients using Stokes' law, (2) the inertia of the drag point is neglected, (3) the isotropic membrane is expressed by changing the equilibrium lengths of the springs inside the erythrocyte model and (4) a dilute suspension of erythrocytes and plasma is assumed, and interactions between erythrocyte models are neglected (although they do interact through the velocity variation in the continuum phase). If the number of drag points is increased, it is possible to imitate the biconcave shape of an actual erythrocyte. However, a large number of drag points requires a high computational load, which is not the purpose of our research. The bead-spring model is required to express the particle stress tensor generated by the erythrocyte, avoiding a high computational load, which was demonstrated in the former studies[15, 16].

The major axis of the octahedron (see figure 1), l_1, is set as $1.3D$ and the minor axis, l_2, is set as one-third of l_1, where D is the erythrocyte diameter. The equilibrium length of each spring is given so that the springs generate no force under the natural conditions shown in figure 1. The drag force acting at the drag point is calculated as the sum of the force acting at the drag point and one-sixth of the force acting at the center of gravity of the erythrocyte model by assuming Stokes' law. The drag coefficients at the drag point are given as $K_n = K_h = 1.13D$, and the drag coefficients at the center of gravity are given as $K_n = 1.5D$, $K_h = 0$, where subscripts n and h denote the major and minor axis directions, respectively. The total drag coefficients of the erythrocyte model are derived as follows; $K_n = 8.28D$, $K_h = 6.78D$, $L_n = 1.91D^3$ and $L_h = 1.06D^3$, where L is the drag coefficient against the rotation. These values are similar to the drag coefficients of an elliptic body ($K_n = 8.28D$, $K_h = 6.78D$, $L_n = 1.91D^3$, $L_h = 1.38D^3$), for which the major axis is D and the minor axis is $D/3$. Therefore, the erythrocyte model generates a drag force similar to that of an actual erythrocyte.

There are three springs inside the erythrocyte model in figure 1, and their lengths change with the deformation of the erythrocyte model. Since it was reported that an

erythrocyte showed tank-tread motion even under a small shear rate[17, 18], the membrane of the erythrocyte is considered to be isotropic. In the present model, the isotropic membrane is expressed by passively changing the equilibrium lengths of these inside springs. The three inside springs are called *sp1*, *sp2* and *sp3*, respectively, in increasing order of shortness. A coefficient C_{sp} is calculated from l_{sp1} and l_{sp2} as $C_{sp} = \max(0, 1 - 0.5 l_{sp2} / l_{sp1})$, where l_{sp1} and l_{sp2} are the lengths of *sp1* and *sp2*, respectively. Then, the equilibrium lengths of *sp1* and *sp2* are given as follows.

$$l_{sp1,0} = (1 - C_{sp}) l_2 + C_{sp} l_1 \quad , \qquad l_{sp2,0} = (1 - C_{sp}) l_1 + C_{sp} l_2 \ . \tag{1}$$

Using this equation, the equilibrium lengths of *sp1* and *sp2* change smoothly with the deformation of the erythrocyte model.

The normal unit vector of the erythrocyte model **n** is also calculated using C_{sp} as

$$\mathbf{n} = \frac{(1 - C_{sp})\mathbf{n}_1 + C_{sp}\mathbf{n}_2}{|(1 - C_{sp})\mathbf{n}_1 + C_{sp}\mathbf{n}_2|}, \tag{2}$$

where $\mathbf{n}_1$ and $\mathbf{n}_2$ are the unit vectors of *sp1* and *sp2*, respectively. Using this equation, the normal vector of the erythrocyte model also changes smoothly with the deformation of the erythrocyte model. The motion of the present model in a simple shear flow is discussed by Ishikawa *et al*. (2003) [16], and the model showed a smooth tank-treading motion.

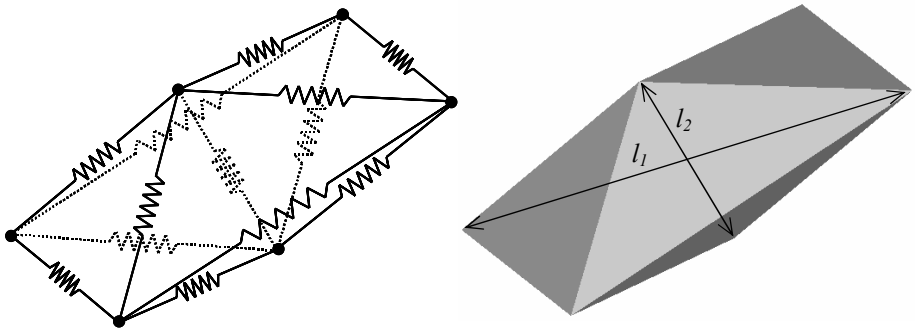

(a) schema of erythrocyte model (b) imaginary appearance of model

Fig.1 Bead-spring model of erythrocyte

2.2 Basic equations

Since in this research the blood is assumed to be a dilute suspension of erythrocytes and plasma, the interactions between erythrocyte models are neglected. The governing equation for a drag point *i* in an erythrocyte model is given as:

$$1.13\mu D(\mathbf{u}_i - \mathbf{v}_i) + \frac{1.5\mu D}{6}\{(\mathbf{u}_g \cdot \mathbf{n} - \mathbf{v}_g \cdot \mathbf{n})\mathbf{n}\} = \sum_j^5 \left\{ \frac{\mathbf{r}_i - \mathbf{r}_j}{|\mathbf{r}_i - \mathbf{r}_j|} k(l - l_0) \right\}, \tag{3}$$

where **r** is the position vector and **v** is the velocity of a drag point, **u** is the velocity of the solvent fluid calculated by equation (4). μ is the viscosity, k is the spring constant, and subscript g denotes the center of gravity. The left side expresses the drag force, which is the sum of the force acting at the drag point and one-sixth of the force acting at the center of gravity of the model. The drag force is calculated from the drag coefficients by assuming Stokes' law. The right side of the equation expresses the spring force, where subscript j is the drag point connected with point i by the spring, and l_0 is its equilibrium length.

The coefficients 1.13 and 1.5 are given so that the erythrocyte model generates a drag force similar to that of an actual erythrocyte, as explained in section 2.1. The spring constant k is given as 5.0×10^{-6} N/m. It is confirmed that the deformation of the erythrocyte model with these parameters corresponds well with experimental results by Bessis and Mohandas[19] (cf. Ishikawa *etal*., 2003 [16]). These coefficients also affect the stresslet, eventually the particle stress tensor given by equation (5). We also confirmed that the shear

thinning property of the present model is consistent with the former continuum model, such as Casson model[5].

The governing equation for the plasma is given by

$$\rho\frac{\partial \mathbf{u}}{\partial t}+\rho(\mathbf{u}\cdot\nabla)\mathbf{u}=-\nabla p+\mu\nabla^2\mathbf{u} -\frac{1}{\Delta V_i}\sum_{m=1}^{\Delta N_i}C_{m,i}\left[1.13\mu D(\mathbf{u}_m-\mathbf{v}_m)+\frac{1.5\mu D}{6}(\mathbf{u}_g\cdot\mathbf{n}-\mathbf{v}_g\cdot\mathbf{n})\mathbf{n}\right], \quad (4)$$

where ρ is the density, p is the pressure, ΔV_i is the volume of computational cell i for the flow field and ΔN_i is the number of drag points in ΔV_i. $C_{m,i}$ is the weight function of drag point m in computational cell i, which satisfies $\sum_{i}^{all}C_{m,i}=1$. (The detailed form of $C_{m,i}$ will be explicitly given in the next section.) The last term in equation (4) denotes the reaction from the erythrocyte models in ΔV. Thus the equation inside the parentheses [ ] is exactly the same as the left hand side of equation (3). By solving equations (3) and (4) simultaneously (two-way coupling), it is possible to simulate a blood flow without using a constitutive equation. The cell models weakly interact through the change in the velocity field given by (4).

The particle stress tensor generated by the erythrocytes can be written as[15]

$$\tau_{ij}=\sum_m\frac{F_{i,m}l_{j,m}Hct}{100V_e}, \quad (5)$$

where V_e is the volume of the erythrocyte, **F** is the force acting on the spring, and *Hct* is the hematocrit.

2.3 Numerical methods

A low-hematocrit blood flow in a small artery with a stenosis is simulated. The computational region is 160 μm in height, 800 μm in length and 8 μm in width as shown in figure 2. Initially, thousands of erythrocyte models are randomly put into the flow field with random attitudes. Then, the motion of the erythrocyte models and the flow field are computed simultaneously. The flow field is assumed to be two-dimensional, on the other hand, the motion of the erythrocyte models is calculated three dimensionally. In this simulation, the time-averaged physical quantities in the suspension are discussed, so it is possible to treat the flow field as two-dimensional. If the instantaneous velocity disturbance is discussed, for instance, the flow field has to be treated three dimensionally. Equation (3) is solved by a fourth-order-accuracy Runge-Kutta scheme and equation (4) is solved by an implicit Euler scheme. After a certain period of simulation, the velocity distribution of the flow field converged. The computation is continued until this convergence is obtained.

The accuracy of the present numerical method has been discussed in some of former studies. The particle stress tensor generated by the erythrocyte model in a simple shear flow is discussed in Ishikawa *etal*. (2001)[15], in which the particle stress tensor and the deformation of erythrocyte model agreed well with the analytical results and former experimental results. The elasticity of a suspension of erythrocyte model was discussed in Ishikawa *etal*. (2001)[20], in which the complex viscosity qualitatively agreed well with the former experimental results. Two way coupling of equations (3) and (4) were first applied to a Poiseuille flow between flat plats[21]. The results showed that the velocity profile without erythrocyte model had numerical error less than 0.1%. In the present paper, the computation was carried out until the error in the continuity equation becomes smaller than 10^{-3} in the dimensionless form.

The computational mesh used in this study is shown in figure 3. In order to satisfy the continuity equation accurately, we generate a fine mesh near the wall. The weight function in equation (4) is calculated as $C_{m,i}=A_i/(16\pi)$, where A_i μm^2 is the area of computational cell i in the x-y plane within the circle of 4 μm radius from drag point m. At the inlet, the

velocity distribution is given as a parabolic shape, and the erythrocyte model flows into the computational domain with random y- and z-positions and a random attitude. We put a cell model at the inlet when one cell flows away at the outlet: thus, the total number of cell models is constant in the computational domain. At the outlet, zero pressure is assumed, and the erythrocyte models flow away. On the wall, the drag point of the erythrocyte model is assumed to show nonelastic and frictionless collision, i.e., the drag point slip on the wall, the rebounding and the friction between the drag point and the wall are neglected. For erythrocyte models, periodic boundary conditions are assumed in the z-direction.

The particle stress tensor is proportional to the volume fraction of particles in a dilute regime, and the next-order term is its square[22]. Thus, the rheological contribution due to cell-cell interaction is about one-tenth of that due to a single cell if one uses a hematocrit of 10% in the simulation. Throughout this study, we used the hematocrit of 10%. The diameter of the erythrocyte D, and the volume of the erythrocyte V_e are given as 8μm and 90μm^3, respectively[23, 24]. The viscosity and the density of plasma are given as 1.5×10^{-3} Pa.s and 1.03×10^3 kg/m^3, respectively. The spring constant of the erythrocyte model is given as 5.0×10^{-6} N/m. By considering the actual blood flow in a vessel with the diameter of 160μm, we can assume that the Reynolds number (Re) is in the order on one. Thus, we used the parameter range Re = 1-5 in this study.

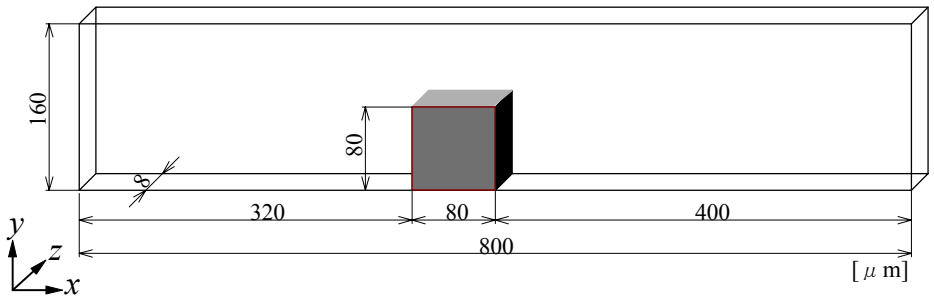

Fig.2 Geometry of computational domain

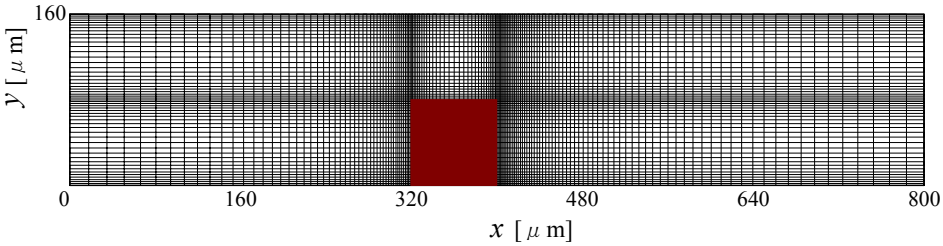

Fig.3 Computational mesh in x-y plane

3. Results and Discussions

3.1 Flow fields

The numerical simulation of blood flows with Hct = 10% in a small artery with a stenosis is performed with Re = 1, 3 and 5, where Re is based on the height of the channel and the mean velocity at the inlet. The streamlines and erythrocyte models of Re = 1 and 5 cases are shown in figure 4. We see that the erythrocyte models are not deformed so much in the case of Re = 1, on the other hand, that with Re = 5 case are deformed considerably around the stenosis. This is because the erythrocyte models in Re = 5 case experience stronger viscous force from the bulk flow than those in the Re = 1 case.

Figure 5 shows the shear stress and pressure distribution along the upper wall when Re = 1. The results are compared with the Hct = 0% case, in which only the plasma phase is

solved without any erythrocyte models. It is found that the shear stress and pressure gradient slightly increase as *Hct* increases. This is because the apparent viscosity of blood increases with increasing *Hct*; thus, the pressure loss in the channel increases under the same flow rate conditions. Since the integration of wall shear stress should balance to the pressure decrease, by considering the balance of forces acting on the channel, the wall shear stress increases with increasing *Hct*. Such non-Newtonian properties of blood affect the flow field more apparently when viscous forces are dominant in the flow field, i.e., low *Re* flows. Figure 6 shows the effect of *Re* on the ratio of inlet pressure with *Hct* = 10% to that with 0%. It is found that the ratio of inlet pressure increases as *Re* decreases, which indicates that the effect of erythrocytes is more significant in small *Re* flows.

Streamlines in the separated region downstream of the stenosis are shown in figure 7, in which the stream lines are drawn in the same interval. We see that the size and strength of the separated region decrease as *Hct* increases. This is because the erythrocytes increase the apparent viscosity in the separated region, and the vortex is weakened by the strong viscous forces. We draw a plot similar to that in figure 6, but in this case we show the size and strength of the separated region. The effects of *Re* on the ratios of vortex strength and separated length with *Hct* = 10% to those with *Hct* = 0% are shown in figure 8. It is found that the ratios of both vortex strength and separated length increase as *Re* decreases, which again indicates that the effect of erythrocytes is more significant in small *Re* flows. This conclusion is consistent with previous studies for a blood flow in a large artery obtained using the bi-viscosity model and the pseudo-Casson model[1, 2].

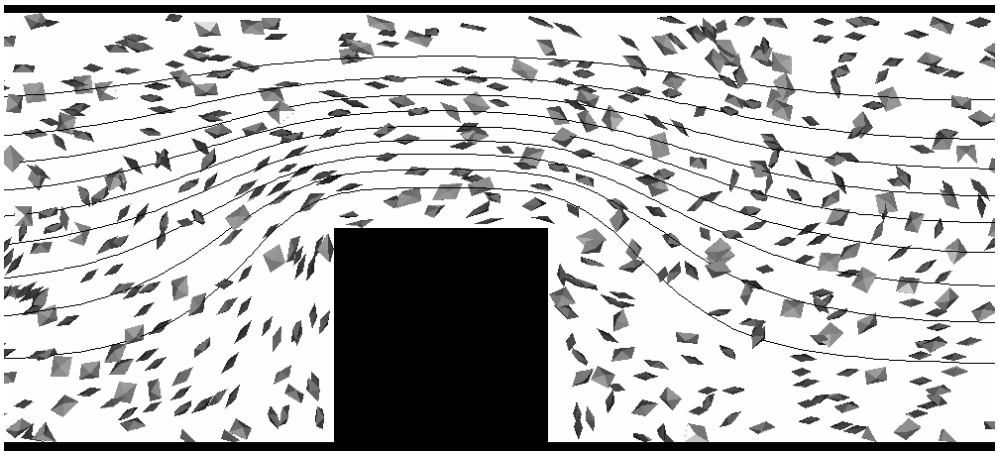

(a) *Re* = 1

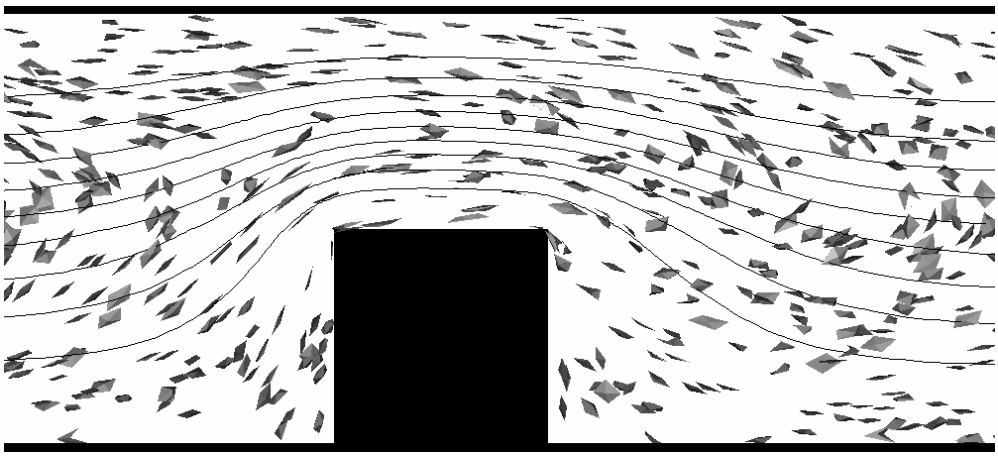

(b) *Re* = 5

Fig.4 Effect of *Re* on the flow fields and the deformation of erythrocyte models

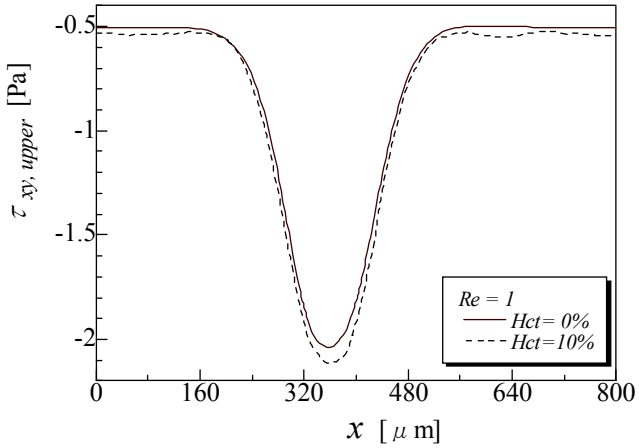

(a) wall shear stress

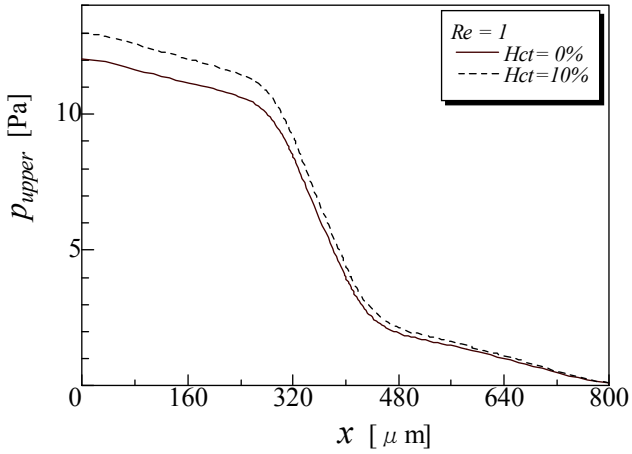

(b) pressure

Fig.5 Effect of *Hct* on the wall shear stress and the pressure on the upper wall

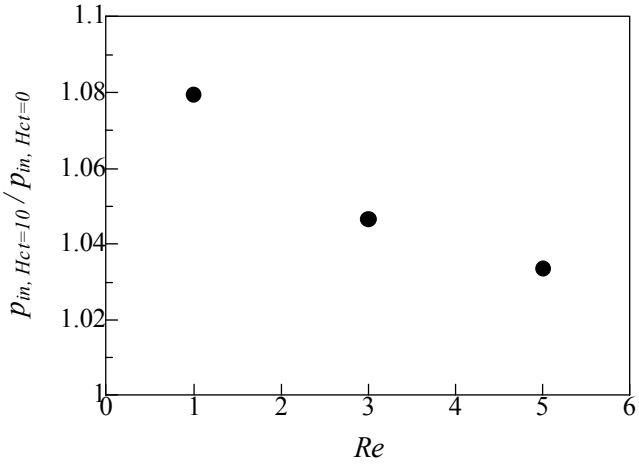

Fig.6 Effect of *Re* on the ratio of inlet pressure with *Hct* = 10% to that with 0%

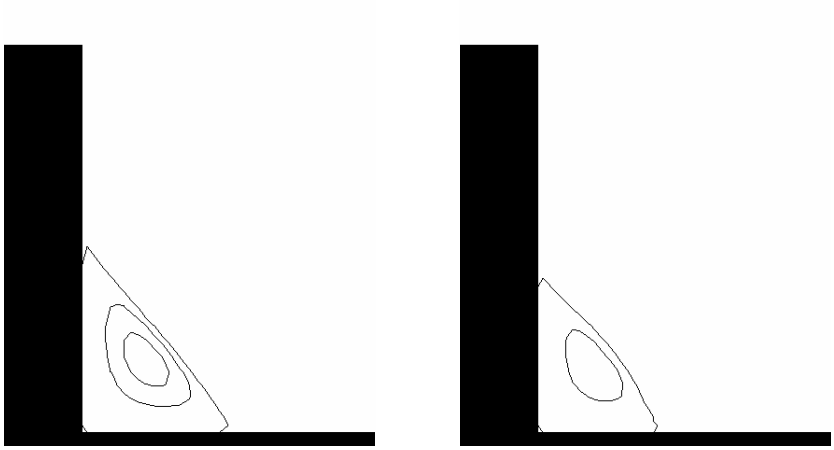

(a) Hct = 0% (b) Hct = 10%

Fig.7 Stream lines in a separated region with Hct = 0 and 10% (Re = 1)

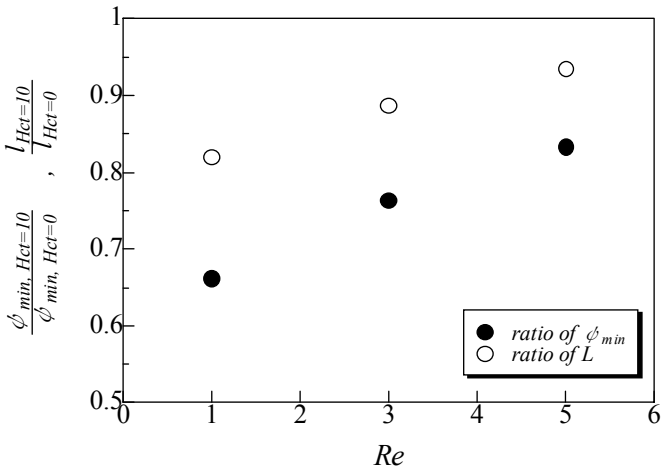

Fig.8 Effect of Re on the ratio of vortex strength and separated length with Hct = 10% to those with Hct = 0%

3.2 Stress fields

A bead-spring erythrocyte model deforms in a simple shear flow, and the deformation showed a good agreement with experiments[15, 16]. When the erythrocyte model flows through the stenosis, it experiences an extensional flow as well as a shear flow. Moreover, the flow fields around the erythrocyte model changes with time as it passes through the stenosis. In such a case, the elasticities of the fluids play an important role in the flow field. Ishikawa *et al.*[23] investigated the elastic properties of a suspension of bead-spring models, and showed that the model could consistently express the elasticity of dilute blood. Actually, the flow of visco-elastic fluids through a stenosis is a troublesome problem if one uses constitutive equations. The constitutive equations of visco-elastic fluids usually have a hyperbolic shape, so they are very difficult to solve numerically without artificial numerical diffusion. If one uses a bead-spring model, one can easily treat the visco-elastic property of fluids, which is an advantage of the present method.

Figure 9 shows the distribution of the maximum value of l_{sp3} / $l_{sp3,0}$ during the computation, where $l_{sp3,0}$ is the equilibrium length of longest inner spring in the erythrocyte model. When an erythrocyte model experiences no induced flow, l_{sp3} / $l_{sp3,0}$ = 1; whereas when the model is stretched, it becomes larger than unity. We see from the figure that the

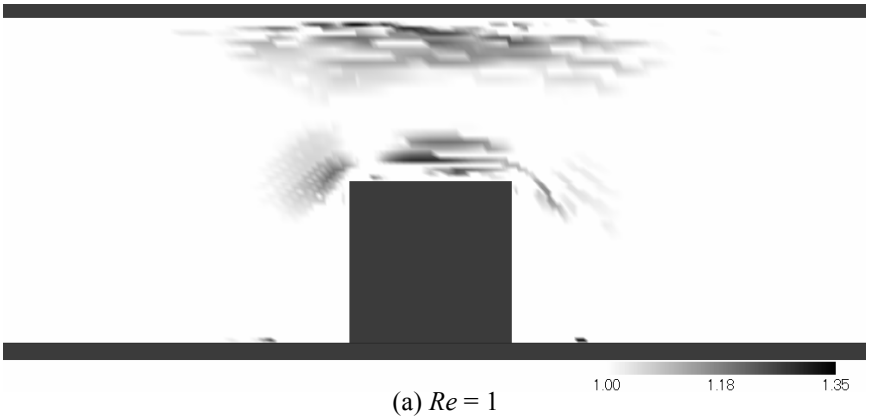

(a) $Re = 1$

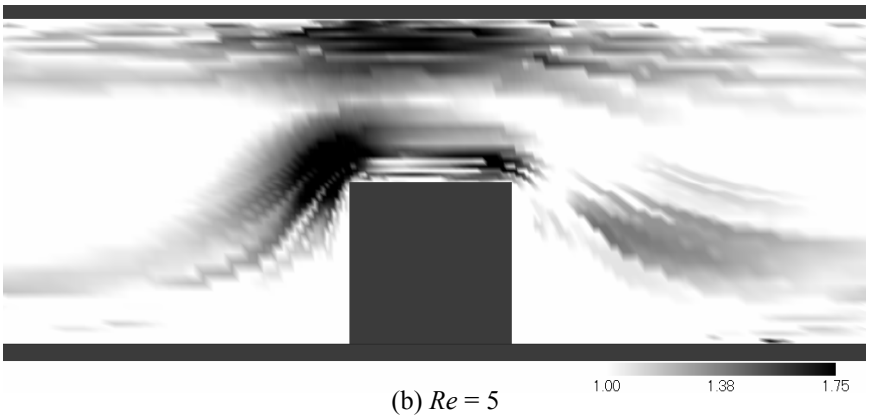

(b) $Re = 5$

Fig.9 Distribution of maximum value of $l_{sp3} / l_{sp3,0}$ during computation

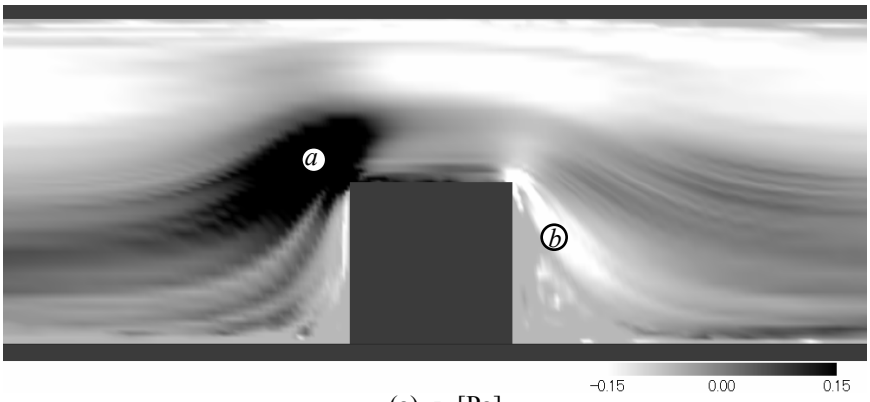

(a) τ_{xy} [Pa]

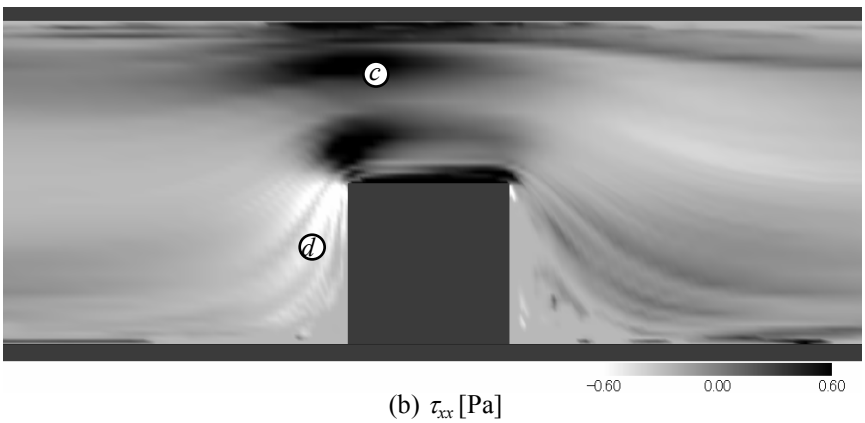

(b) τ_{xx} [Pa]

Fig.10 Distribution of particle stress tensor due to erythrocyte models ($Re = 5$, $Hct = 10\%$)

deformation increases as *Re* is increased. Because the shear rate and extensional rate increase as *Re* is increased, a large deformation appears around the stenosis, where a high shear rate is induced because of the jet flow at the constriction. We see in figure 9(b) that the deformation is larger upstream than downstream of the stenosis. This is because the extensional rate is lower downstream, where there is a separated region and the flow does not expand fully just after the stenosis. Since the deformation of erythrocytes is an important quantity in discussing the burst phenomena of a cell, we can say that this numerical method has an advantage compared with using constitutive equations.

It is also important to discuss the particle stress tensor in order to understand the flow field of non-Newtonian fluids. Figure 10 shows the time-averaged *xy* and *xx* components of the particle stress tensor with $Re = 5$ and $Hct = 10\%$. We see a large τ_{xy} at point *a* in figure 10(a), and a small τ_{xy} at point *b*. This kind of stress field can be easily understood if one looks at the deformation of the erythrocyte models at each point. Figures 11(a) and (b) show the deformation of the erythrocyte models at points *a* and *b*, respectively. At point *a*, the model is stretched in the direction of $y = x$, so it generates a positive τ_{xy}. At point *b*, on the other hand, the model is stretched in the direction of $y = -x$, so it generates a negative τ_{xy} in this case.

In figure 10(b), we see a large τ_{xx} at point *c* and a small τ_{xx} at point *d*. This can be explained by the deformation of the erythrocyte models at points *c* and *d* (see figures 11(c) and (d)). At point *c*, the model is stretched in the *x* direction, so it generates a strong first normal stress difference. At point *d*, on the other hand, the model is stretched in the *y*-direction, so it generates a negative first normal stress difference, but a positive second normal stress difference. Another advantage of the present numerical method is that the stress field can be easily understood by considering the deformation of the erythrocyte models.

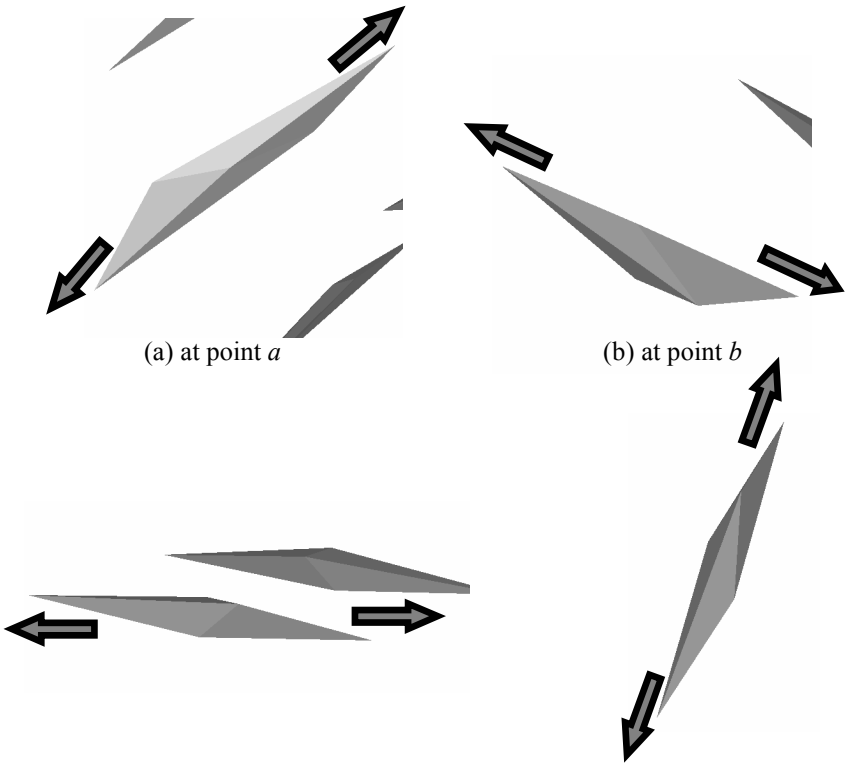

(a) at point *a* (b) at point *b*

(c) at point *c* (d) at point *d*

Fig.11 Behavior of erythrocyte models at points *a*, *b*, *c* and *d*.

4. Conclusions

In this study, a bead-spring erythrocyte model is used to simulate a low-hematocrit blood flow through a small artery with a stenosis. It is found that the effects of erythrocytes are considerable in small *Re* flows, which are as follows: (a) the wall shear stress and the pressure gradient increase as *Hct* is increased, and (b) the strength of the separated vortex and the length of the separated region decrease as *Hct* is increased. We have also discussed the stress field due to the deformation of the erythrocyte models. The results show that the present model can express the shear thinning property and the elasticity of blood. Significant deformation of the erythrocyte models appears around the stenosis, and the deformations are slightly greater in the upstream side. Since the deformation of erythrocytes is an important quantity in discussing the burst phenomena of a cell, we can say that this numerical method has an advantage compared with using constitutive equations. Another advantage of the present numerical method is that the stress field can be easily understood by considering the deformation of the erythrocyte models.

Acknowledgement

This research was supported by Grant-in-Aid for Young Scientists (B) No.17760137

References

(1) Ishikawa T., Guimaraes L. F. R., Oshima S. and Yamane R., *Fluid Dyn. Res*., 22 (1998), 251-264
(2) Ishikawa T., Oshima S. and Yamane R., *Fluid Dyn. Res*., 26 (2000), 35-52
(3) Nakamura, M. and Sawada, T., *J. Biomech. Eng*., 110 (1988), 137-143
(4) Luo, X. Y. and Kuang, Z. B., *J. Biomech. Eng*., 114 (1992), 512-514
(5) Casson, N., *Rheology of Disperse System* (1959), Pergamon Press, London
(6) Pozrikidis, C., *J. Fluid Mech*., 440 (2001), 269-291
(7) Pozrikidis, C., *Annals Biomed. Eng*., 31 (2003), 1194-1205
(8) Pozrikidis, C., *Annals Biomed. Eng*., 33 (2005), 165-178
(9) Ladd, A. J. C., *J. Fluid Mech*., 271 (1994a), 285-309
(10) Ladd, A. J. C., *J. Fluid Mech*., 271 (1994b), 311-339
(11) Ladd, A. J. C., *Phys. Fluids*, 9 (1997), 491-499
(12) Sangani, A. S. & Mo, G., *Phys. Fluids*, 8 (1996), 1990-2010
(13) Zinchenko, A. Z. & Davis, R. H., *J. Comp. Phys*., 157 (2000), 539-587
(14) Zinchenko, A. Z. & Davis, R. H., *J. Fluid Mech*., 455 (2000), 21-62
(15) Ishikawa, T., Kawabata, N. & Tachibana, M., *JSME Int. J.,* C (2001), 44, 964-971
(16) Ishikawa, T., Kawabata, N. & Tachibana, M., *Acta Bioeng. Biomech*. (2003), 5, 21-34
(17) Fischer, T. M., Stohr-Liesen, M. and Schmid-Schonbein, H., *Science* (1978), 202, 894-896
(18) Fischer, T. M., *Biophys*. (1980), 32, 863-868
(19) Bessis, M. and Mohandas, N., *Blood Cells* (1975), 1, 307-313
(20) Ishikawa, T., Kawabata, N. and Tachibana, M., *Trans. Jap. Soc. Mech. Eng*., B (2001), 67, 2180-2187 (in Japanese)
(21) Ishikawa, T., Kawabata, N., Sawazaki H. & Tachibana, M., *Conference on Modelling Fluid Flow* (2003), 567-572
(22) Batchelor, G. K. & Green, J. T., *J. Fluid Mech*. (1972), 56, 401-427
(23) Evans, E. and Fung, Y. C., *Microvascular Res.* (1972), 4, 335 - 347
(24) Roe, E. W., Edward, W. M. and Henry G., *Trans. Soc. Rheology* (1962), 6, 19-24